https://doi.org/10.5194/egusphere-2026-3919
Preprint. Discussion started: 3 August 2026

Evaluating N_2O Analyzers for Urban Monitoring: Evidence for Underestimated Emissions

Andrew Hallward-Driemeier[1], Raghav Dhall[1], Yuwei Zhao[1], and Róisín Commane[1,2]

[1]Department of Earth and Environmental Sciences, Columbia University, New York, NY, USA
[2]Lamont-Doherty Earth Observatory, Columbia University, Palisades, NY, USA

Correspondence: Andrew Hallward-Driemeier (ah3956@columbia.edu)

Abstract. Nitrous oxide (N_2O) is a potent greenhouse gas and ozone-depleting substance. Approximately 42% of anthropogenic N_2O emissions are thought to be emitted from urban areas. We tested three N_2O analyzers for their suitability to measure N_2O in urban areas from tower and mobile platforms. All three analyzers (Aerodyne SuperDUAL, Aeris MIRA Ultra, and LI-COR LI-7820) have sufficient precision for urban measurements but require different amounts of calibration and attention for best results. Using these analyzers, we observed tower-level enhancements at least 3 times larger than predicted from the best available inventory for the NYC region. Co-measurement of carbon monoxide (available on all but the LI-7820) were used to identify combustion-related enhancements of N_2O. Mobile driving confirmed that traffic related emissions for NYC are captured by the inventory and that wastewater treatment is the most likely source for the missing N_2O emissions.

1 Introduction

Nitrous oxide (N_2O) is a potent greenhouse gas with a global warming potential 273 times greater than that of carbon dioxide (CO_2) and is responsible for approximately 6% of anthropogenic global warming to date (Forster et al., 2023; Szopa et al., 2023). Nitrous oxide has a lifetime of over 100 years in the atmosphere, with the dominant loss pathways including reaction with $O(^1D)$ and photolysis in the stratosphere (Prather et al., 2015). The reaction of N_2O with $O(^1D)$ produces nitrogen oxide (NO), which catalyzes the destruction of ozone in the stratosphere (Crutzen, 1970). As emissions of nitrous oxide rise and emissions of other ozone depleting substances, such as CFCs, decline, nitrous oxide has become the dominant anthropogenic ozone depleting substance in the 21st century (Ravishankara et al., 2009). Unlike other important ozone depleting substances, the Montreal Protocol does not regulate N_2O.

Global N_2O emissions are an estimated 18.3 Tg yr^{-1}, with a change in atmospheric abundance of 4.6 Tg yr^{-1}. Approximately 36% of N_2O emissions are anthropogenic, with agriculture the largest source (3.6 Tg yr^{-1}) (Tian et al., 2024). Fossil fuels and industry together emit 1.1 Tg yr^{-1}. According to the EDGARv2024 inventory (described below), urban areas (defined by Schiavina et al. (2023) as urban center, dense urban cluster, or semi-dense urban clusters) account for 42% of total anthropogenic N_2O emissions. Traffic (Jimenez et al., 2000; Chu et al., 2024), wastewater treatment and sewers (Townsend-Small et al., 2011; Fries et al., 2018; Vasilaki et al., 2019; Song et al., 2024), recreational use (Barker et al., 2022; Charoenpornpukdee et al., 2023; Forster et al., 2026), and soils (Järvi et al., 2014; Pierre et al., 2016; Zhan et al., 2023) have been identified as

https://doi.org/10.5194/egusphere-2026-3919
Preprint. Discussion started: 3 August 2026

important urban sources. Addington et al. (2021) found a factor of 3 underestimation of urban N_2O emissions in Los Angeles using a long path laser system, consistent with previous findings from Wunch et al. (2009). Aircraft measurements in Rotterdam also found a factor of 3 underestimate in inventories linked to both traffic and wastewater treatment (Tong et al., 2023, 2025). However, aircraft measurements in the San Joaquin Valley found that traffic emissions were overestimated (Herrera et al., 2021). Tower-based measurements in the suburbs of Zurich were consistent with inventory emissions estimates(Harris et al., 2017). Traffic emissions have become a larger source due to the use of catalysts, used to reduce NO_x emissions, that increase N_2O emissions (Hoekman, 2020). Traffic and other fossil fuel combustion also emit carbon monoxide (CO) as a combustion by-product, while other sources do not emit CO. Therefore, CO can be used to distinguish combustion-related N_2O emissions from other sources.

N_2O emissions have been characterized in New York City (NYC) from traffic, most likely buses (see Supporting Information S7), and urban soils (Pierre et al., 2016). NYC has fourteen wastewater treatment plants (WWTP), along with several others in the suburbs, though sludge de-watering and storage occur at only a handful of these plants. Several studies have identified large N_2O emissions from biological nutrient removal processes (Desloover et al., 2012; Law et al., 2012; Massara et al., 2017) and sludge storage (Oshita et al., 2014; Willén et al., 2016; Gålfalk et al., 2022; Gålfalk and Bastviken, 2025) and de-watering (Oshita et al., 2014).

The laser-based N_2O analyzers we will investigate here have been used for tower networks (Miller et al., 2012; Ganesan et al., 2015; Bergamaschi et al., 2015) and static chamber sampling (Brannon et al., 2016; Richardson et al., 2022; Kong et al., 2025; Yang et al., 2025). N_2O analyzers are capable of operating on different mobile platforms, depending on their configuration; all of the analyzers can operate on mobile vehicle measurements (Moore et al., 2025), but only a few can be used for airborne measurements (Xiang et al., 2013; Gonzalez et al., 2021; Knez et al., 2026). For tower and airborne applications especially, the diffuse nature of N_2O emissions means that enhancements are often below 3 parts per billion by volume (ppbv), or 1% of the background (Xiang et al., 2013; Haszpra et al., 2018). Accurately measuring N_2O in these settings therefore requires high precision analyzers.

In this paper, we evaluate three commercially available nitrous oxide analyzers and demonstrate the importance of making urban measurements with these or other similar analyzers. The analyzers were (i) a mid-infrared (IR) absorption spectrometer (Aeris Technologies MIRA Ultra LDS) [Aeris MIRA Ultra], (ii) a cavity-enhanced IR absorption spectrometer (Aerodyne Research Inc. SuperDUAL QCL/ICL) [Aerodyne SuperDUAL], and (iii) an optical feedback-cavity enhanced absorption spectrometer (LI-COR Environmental LI-7820) [LI-7820]. The Aeris MIRA Ultra and Aerodyne SuperDUAL analyzers also measure CO, while the LI-7820 does not. We tested the response of each of these analyzers to water vapor and compared their suitability for stationary and mobile setups. We then demonstrated the ability of these analyzers to distinguish between multiple sources of N_2O and estimate total N_2O emissions for the NYC region.

https://doi.org/10.5194/egusphere-2026-3919
Preprint. Discussion started: 3 August 2026

2 Methods

2.1 Description of Analyzers

2.1.1 Aeris Technologies MIRA Ultra LDS

The Aeris Technologies MIRA Ultra LDS (product no. 100490) analyzer measures N_2O, CO, and H_2O using a mid-IR laser. This analyzer has been used for stationary deployments (Krebbers et al., 2025) and floating chamber studies (Peterse et al., 2024). Aeris Technologies produces a similar analyzer measuring N_2O and CO_2 that has been used for short-term deployments near emissions sources (Kashtan et al., 2023, 2024; Chu et al., 2024) and soil chamber studies (Triches et al., 2025; Aumer et al., 2025) Aeris Technologies, Inc. estimate the precision of the MIRA Ultra analyzer at 500 parts per trillion by volume (pptv) for both N_2O and CO.

The analyzer requires an external computer to transmit data, run solenoids for calibrations, and keep the time synced. It has an internal pump with a flow rate of around 300 standard cubic centimeters per minute (sccm) through a 60 cubic centimeter cell. The internal clock on our analyzer drifted by 40 seconds over the course of the three week tower deployment. Our analyzer comes with a rack mount and a small footprint (48 cm x 18 cm x 28 cm; 9 kg).

We have previously observed the Aeris MIRA Ultra report non-physical negative CO mole fractions due to a line-locking issue in the software. This problem required a visit to manually reset the analyzer. However, the issue did not appear to affect the N_2O measurements. This issue most commonly occurs during instrument setup where it was quickly corrected but has occurred twice in the middle of a field deployment over the past three years. This poses a significant concern for long-term deployments of the Aeris MIRA Ultra, especially at sites without internet access or that are difficult for technicians to reach. The Aeris MIRA Ultra did not experience this issue while the analyzers were deployed together.

2.1.2 Aerodyne Research Inc. SuperDUAL

The Aerodyne SuperDUAL has been deployed for previous tall-tower (McKain et al., 2015; Schiferl et al., 2024, 2025), mobile vehicle (Yacovitch et al., 2014; Catena et al., 2026), aircraft (Kostinek et al., 2019; Plant et al., 2019) measurements, and flask sampling (Tong et al., 2023, 2025). Our analyzer has a 2L astigmatic Herriott cell with a path length of 210 m. It was manufactured in 2015, and had both lasers and the computer replaced between 2020 and 2023. The internal computer on the Aerodyne SuperDUAL allows it to connect to the internet, control solenoids, and maintain a stable time. The first laser is an Interband Cascade Laser (ICL) that sweeps from 2988.520 to 2990.625 cm^{-1} to detect methane, ethane, and H_2O. The analyzer's main H_2O measurement, and the one used in this paper, comes from the ICL. The methane and ethane measurements of this analyzer have been extensively described in Commane et al. (2023). The second laser is a Quantum Cascade Laser (QCL) to measure dry mole fractions of N_2O, carbon dioxide (CO_2), and CO. The QCL sweeps from 2227.550 to 2228.000 cm^{-1} and includes absorption features for $^{13}CO_2$ (2227.605 cm^{-1}), CO (2227.639 cm^{-1}), N_2O (2227.843 cm^{-1}), and H_2O. We implemented the water broadening coefficients recommended by Kostinek et al. (2019) for this analysis. Aerodyne Research

https://doi.org/10.5194/egusphere-2026-3919
Preprint. Discussion started: 3 August 2026

Inc. did not estimate the precision of the analyzer, but Kostinek et al. (2019) estimated the precision at 45 pptv for N_2O and 1.3 ppbv for CO.

The Aerodyne SuperDUAL is best suited for long-term tower or mobile lab sampling. It is large and heavy (56 cm × 77 cm × 64 cm; 75 kg) and requires an external pump and chiller (to maintain laser temperature stability) that require a stable power source. The analyzer can run at up to 10 Hz sampling frequency for eddy covariance applications but sampled at 1 Hz for our application. The external pump allows customization of the flow rate through the analyzer for higher frequency applications. Our analyzer was configured for a flow rate of around 1500 sccm. Aerodyne Research Inc. recommends frequent (up to once per hour) calibration of the analyzer to account for small temperature changes in the lasers. This analyzer has many options for customization that require expert maintenance of the wavelength fitting and mirror alignment for optimal use.

2.1.3 LI-COR Environmental LI-7820

The LI-COR Environmental LI-7820 has been used primarily for static chamber studies (Richardson et al., 2022; Yang et al., 2025; Kong et al., 2025; Seuferling et al., 2025; Bai et al., 2025). It measures only N_2O and H_2O but does not provide an absorption wavelength range. LI-COR Environmental estimate the precision of the LI-7820 at 400 pptv for N_2O.

The LI-7820 is slightly larger than the Aeris MIRA Ultra analyzer (51 cm x 18 cm x 33 cm; 11 kg). However, unlike the other two analyzers it has 8 hours of battery life and a handle for easy transport, making it ideal for applications without access to stable electricity, such as car, backpack, or chamber sampling. The analyzer also has an internal pump with a flow rate of about 250 sccm. The optical cell is the smallest of the analyzers, at 6.41 cubic centimeters. The LI-7820 also requires an external computer to download or transfer data, control solenoids, and keep the time synced. The clock on the LI-7820 drifted by 90 seconds over the 3-week tower deployment.

2.2 Analyzer Testing

We performed three tests on each of the analyzers, measuring their precision, response to humidity changes, and stability. To test the precision, we continuously sampled a dry compressed-air cylinder for four hours and calculated the Allan-Werle variance (Yver Kwok et al., 2015; Defratyka et al., 2021). The Allan-Werle variance indicates the precision of the analyzers as a function of the averaging period. The trough of the curve represents the maximum instrument precision and the time scale over which analyzer drift becomes relevant.

Previous work has shown that similar laser spectrometers often have a residual dependence on humidity (Kostinek et al., 2019; Commane et al., 2023; Knez et al., 2026). To test the response to humidity, we used a Perma Pure Nafion (™) dryer to vary the humidity of the analyzers while sampling from the same compressed air tank used in the precision test. The Nafion dryer has a semi-permeable membrane separating the sample gas from a counter flow of air. This membrane is permeable to water but testing indicated that other gases, especially CO_2, could pass across the membrane for a sufficient gradient. Therefore, we used the same cylinder for the counter flow as the sample flow. We determined the dependence of each analyzer on water vapor from the fit to the reported mole fraction against the reported humidity.

https://doi.org/10.5194/egusphere-2026-3919
Preprint. Discussion started: 3 August 2026

To test the analyzers' stability, we excluded some of the calibration tank runs from our calibration setup and re-interpolated the calibration to those points to estimate how the calibration uncertainty changes as a function of the calibration setup. For example, we applied only every second (or third, or fourth, etc) day's 2-tank span and intercept, keeping the frequency of the compressed air constant. We repeated this test for the intercept, using compressed air runs every four (or six, or eight, etc) hours to interpolate high-frequency intercept changes, keeping the frequency of the 2-tank calibrations constant. For each test, we interpolated the observed value between the used calibrations to the unused calibrations in the same manner as we calibrated the ambient data. We defined the uncertainty due to lower frequency intercept calibrations as the standard deviation of the difference between the calibrations not used and the interpolated value. Results from these tests for CO can be found in Supporting Information S1.

2.3 Tower Deployments

The Aerodyne QCLS was deployed at the City University of New York (CUNY) Next Generation Environmental Sensor Observatory in Harlem (40.8153,-73.9503) from August 2024 to May 2026. The sampling point is 93 m above sea level and 56 m above ground level and has been described elsewhere (Commane et al., 2023; Schiferl et al., 2024, 2025). For three weeks in May 2025 the Aeris MIRA Ultra and LI-7820 measured from this same inlet. Raw data from all analyzers were corrected according to the results of the humidity correction described below. To calibrate the analyzers, we sampled two calibration tanks traceable to the NOAA-2006A standard for N_2O and WMO-X2014A for CO once daily to determine a slope and intercept for calibration. We then interpolated the slope and intercept from the 2-tank calibration to the 1-second raw data. We also sampled a compressed air tank every 2 hours to account for higher frequency changes in the intercept. We then interpolated any intercept changes calculated from the compressed air to the 1-second data after applying the 2-tank calibration.

The Aeris MIRA Ultra was deployed separately at Rutgers University (40.4623,-74.4293, 20 m AGL) and Floyd Bennett Field (FBF; 40.5818,-73.8887, 4 m AGL). These deployments were calibrated once daily with two calibration tanks traceable to the NOAA-2006A standard for N_2O and WMO-X2014A for CO. These deployments did not have the compressed air tank to adjust the intercept every two hours.

2.4 Mobile Deployments

The mobile deployment at street level shown here occurred in January and June of 2025 as part of the Transport and Energy Emissions from Manhattan Streets (TEEMS) campaign. The TEEMS deployments included the Aeris MIRA Ultra and the LI-7820 (June-only). Further details, including survey design and plume identification are described in more detail in Supporting Information S7. The mobile measurements outside of Ward's Island WWTP occurred in January of 2024 and used the Aeris MIRA Ultra. The Aerodyne SuperDUAL has also been deployed in mobile measurements, including in Catena et al. (2026) but required the larger space and greater power supply of a dedicated mobile laboratory. Plumes were identified using CO enhancements and a linear regression was calculated between N_2O and CO for the 20-second period centered on the plume. We identified traffic-related plumes as those with an R^2 for the N_2O/CO regression line above 0.75 and an R^2 for the C_2H_6/CH_4 regression line below 0.9. We also applied this criteria to the 5-minute averaged tower data.

https://doi.org/10.5194/egusphere-2026-3919
Preprint. Discussion started: 3 August 2026

2.5 Observation-Informed Regional Emissions

To estimate total emissions for the region, we scale the sum of an emissions inventory for the region by the ratio of the observed N_2O enhancements to predicted N_2O enhancements using the same inventory (Equation 1). This method is well established for estimating regional emissions of greenhouse gases (Xiang et al., 2013; McKain et al., 2015; Floerchinger et al., 2021; Sargent et al., 2018, 2021; Wei et al., 2022) and has been used previously at this site for methane (Schiferl et al., 2025) and CO emissions (Schiferl et al., 2024).

$$Estimated\ \mathrm{N_2O}\ Emissions = Inventory\ Emissions \cdot \frac{Observed\ Enhancements}{Predicted\ Enhancements} \tag{1}$$

We estimated the background N_2O from a distribution of backgrounds using a set of 240 resampling bootstraps (n=1000) with replacement from the hourly mean observations in each rolling 10 day window. For each set, we took the 30th percentile observation and then took the mean across the sets as our estimated background for that hour and the 25th and 75th percentiles across the sets as the background uncertainty. This method is the same as previous work at this site for methane (Schiferl et al., 2025). We chose to use the 30th percentile observation is intentionally a conservative estimate of the background N_2O mole fraction given the lack of an upwind site to characterize inflow into the region. Studies for other greenhouse gases typically use the 5th percentile at urban sites (Ammoura et al., 2016; Lopez-Coto et al., 2022; Schiferl et al., 2024). Since N_2O is typically thought to have fewer urban sources we opted to use a higher background. Further discussion of the impact of this choice can be found in Supporting Information S2. To reduce uncertainty stemming from the transport model we only included data (11:00 - 16:00 local time) when the boundary layer is highest and well-mixed.

The highest-resolution inventory available for the NYC region is the EDGARv2024 inventory (developed for 2023) at a resolution of 0.1x0.1°(Crippa et al., 2024). According to EDGARv2024, emissions for the NYC region in 2023 were around 6000 metric tons. To estimate the predicted enhancements, we convolve this inventory ($mol \cdot m^{-2} \cdot s^{-1}$) with footprints ($\frac{ppb}{mol \cdot m^{-2} \cdot s^{-1}}$) generated from the Stochastic Time-Inverted Lagrangian Transport model, or STILT (Lin et al., 2003; Fasoli et al., 2018). We configured STILT to release 500 particles backwards in time for 24 hours, driven by meteorology from the High Resolution Rapid Refresh (HRRR, from the National Oceanic and Atmospheric Administration) at 3 km resolution (Benjamin et al., 2016). Tracking the particles' interactions with the bottom half of the boundary layer produces a map of the surface influence on our site called a footprint. We also tested this with meteorology from the North American Mesoscale 3 km (NAM3) forecast from the National Centers for Environmental Prediction for the second year of our analysis. Results are available in Supporting Information S3 and are consistent with the results using HRRR meteorology.

https://doi.org/10.5194/egusphere-2026-3919
Preprint. Discussion started: 3 August 2026

3 Results and Discussion

3.1 Analyzer Testing

3.1.1 Analyzer Precision

All three analyzers outperformed their reported 1-second precision in our tests. The Aerodyne SuperDUAL shows the greatest precision, followed by the LI-7820 and then the Aeris MIRA Ultra (Figure 1A). However, the Aerodyne SuperDUAL has its minimum variance at a shorter integration time, indicating that analyzer drift happens on shorter timescales and that the analyzer may require more frequent calibration to achieve best results.

3.1.2 Humidity Sensitivity

The Aerodyne SuperDUAL shows the greatest sensitivity to water vapor, while the LI-7820 was the most difficult to correct due to its nonlinear response to humidity (Figure 1B).

Using the water broadening coefficients from Kostinek et al. (2019), the Aerodyne SuperDUAL N_2O had a residual humidity dependence of 2.13 $\frac{ppbv}{\%\ H_2O}$. This relationship was linear and simple to correct. After the tower deployment for this study ended, we re-calculated the etalon fit on the Aerodyne SuperDUAL. When we tested the water vapor sensitivity again after changing the etalon fit, the correction had changed significantly, including a sign change for some species. We ran that test multiple times and observed that the humidity correction was consistent when the etalon fit remained constant. Therefore, we conclude that adjustments to the etalon fit will also affect the water vapor broadening and a water vapor test should be run after every etalon adjustment for the Aerodyne SuperDUAL.

The Aeris MIRA Ultra showed a linear dependence on water vapor. The raw N_2O measurement changed by -0.68 $\frac{ppbv}{\%\ H_2O}$ and was simple to correct. We tested the humidity dependence for this analyzer multiple times with consistent results each time. There is an option to manually adjust the spectral fitting in the Aeris MIRA Ultra software, which may affect the humidity dependence, but we did not change this during our deployment.

The LI-7820 showed a cubic dependence on humidity, with changes of up to 0.5 ppbv at 0.3% H_2O and -0.5 ppbv at 1.4% H_2O. However, the cubic fit is imperfect and does not capture the trend as well as the fits for the Aerodyne SuperDUAL and Aeris MIRA Ultra. The LI-7820 also exhibited a hysteresis at around 0.2 % H_2O, with the reported N_2O dropping by around 0.5 ppbv. We did not observe this step change around 0.2% H_2O in the daily calibrations.

3.1.3 Analyzer Calibration

For all three analyzers, assuming a linear calibration with a slope and intercept, changes in the intercept had a larger effect on calibration uncertainty than changes in the slope. None of the analyzers showed a significant change when changing the frequency of the 2-tank span and intercept (while holding the frequency of the compressed air constant at every 8 hours, see Figure 1C). In contrast, all of the analyzers showed a significant dependence on the frequency of the compressed air (holding the 2-tank span constant at every 10 days). The dependence was greatest for the LI-7820, which has the lowest uncertainty

https://doi.org/10.5194/egusphere-2026-3919
Preprint. Discussion started: 3 August 2026

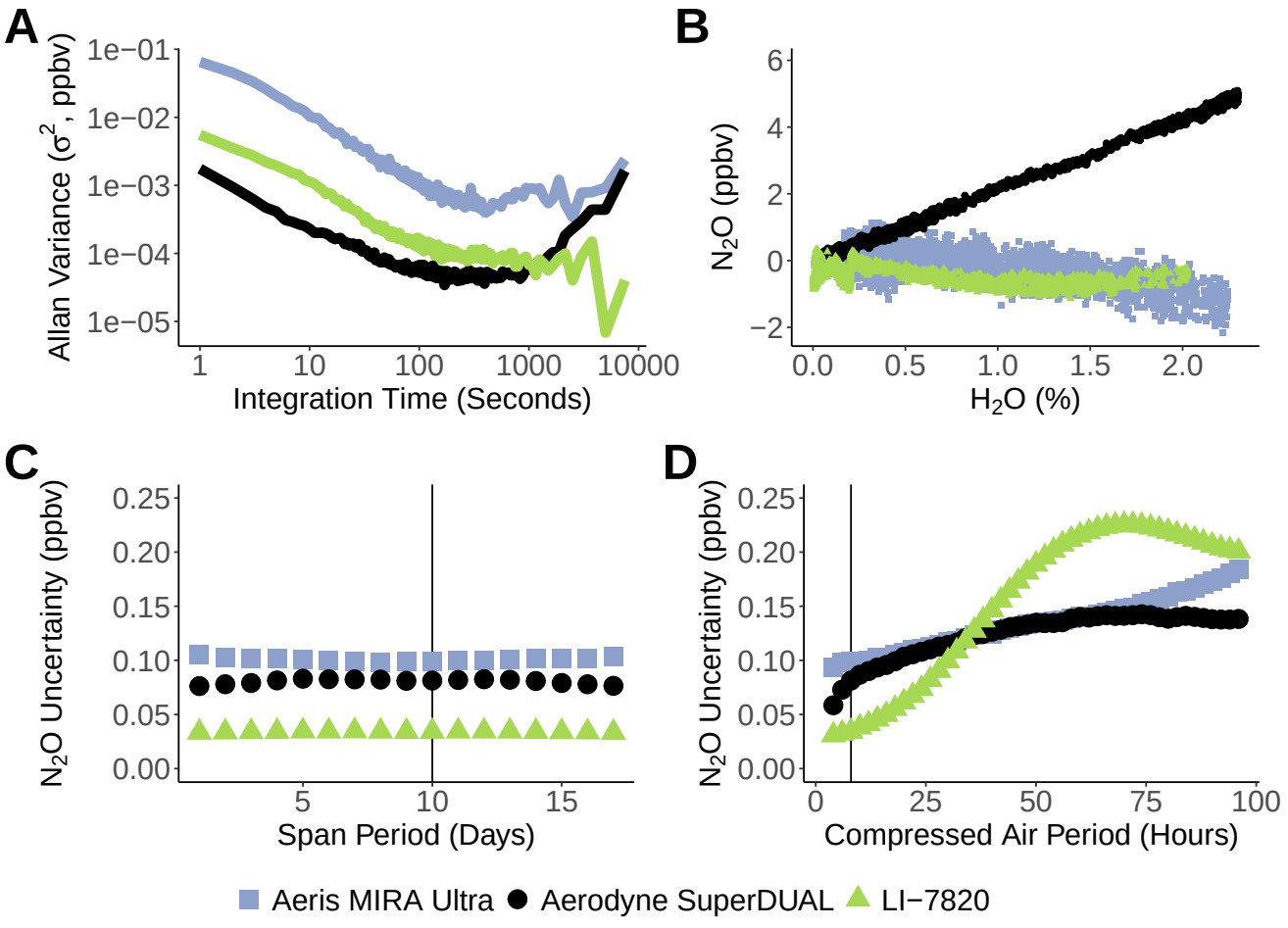

Figure 1. A) Allan-Werle variance plot of N_2O for the Aeris MIRA Ultra (blue), Aerodyne SuperDUAL (black), and LI-7820 (green). B) Humidity dependence of analyzers plotted as raw reported N_2O mole fraction against reported H_2O. C) Uncertainty associated with changing the frequency of the 2-tank span and intercept, holding the compressed air constant at every 8 hours (the vertical line on D)). D) Uncertainty associated with changing the frequency of the compressed air intercept adjustment, holding the 2-tank span and intercept constant at every 10 days (the vertical line on C)).

https://doi.org/10.5194/egusphere-2026-3919
Preprint. Discussion started: 3 August 2026

with frequent calibration but the most uncertainty once the compressed air was sampled less than once per day (Figure 1D). The Aerodyne SuperDUAL consistently performed better than the Aeris MIRA Ultra for N_2O despite the known temperature dependence of the lasers. Calibrating every hour during regular operation, as the manufacturer suggests, would likely result in improved performance from the Aerodyne SuperDUAL.

We observed that the LI-7820 had a wave-like variability in the reported N_2O mole fraction with a period of about 3 days. Adjusting the intercept with the compressed air every 4-12 hours, we were able to fit this variability and the LI-7820 had the lowest uncertainty of the three analyzers. However, when applying the intercept adjustment every 2 days, we were unable to fit this variability and the LI-7820 had greater uncertainty than the other two analyzers. The LI-7820 exhibited a sudden jump in its calibration on May 14^{th} (See Supporting Information S4). This jump occurred during a low-span calibration tank and changed the raw observed N_2O by around 1.5 ppbv. We observed that this jump affected both the slope and the intercept of the two-tank calibration. Neither the Aerodyne SuperDUAL nor the Aeris MIRA Ultra exhibited a similar jump.

3.1.4 Tower Deployment

All three of the analyzers performed within limits sufficient to capture urban N_2O variability. We observed enhancements greater than 100 ppbv in the 1 Hz dataset, well above the noise of all three analyzers. The R^2 between each of the analyzer pairs was above 0.94 for the 1 Hz data after calibration and water correction were applied. The different cell sizes of the analyzers and instrumental noise account for any remaining discrepancies.

3.2 Urban N_2O Observations

3.2.1 Traffic Signals

The TEEMS campaign targeted N_2O emissions from traffic, with a particular bias towards bus emissions, which account for 9-21% of on-road N_2O emissions in NYC (see Supporting Information S7). Figure S5 shows the Aeris and LiCOR sampling a traffic-related plume of N_2O. The different cell sizes lead to slightly different responses to the plume (see Supporting Information S5). While we do not expect the N_2O/CO ratio of traffic and other combustion sources to match exactly, we observed a strong similarity in the observed N_2O/CO ratio at street and tower level. At street level, the median slope was 0.013 $\frac{ppbv\ N_2O}{ppbv\ CO}$ (Inter-quartile range: 0.006, 0.023). Only 11% of observed CO plumes at street level contained N_2O above 5 ppbv, indicating that the majority of vehicles in NYC do not use urea-based catalysts.

At the rooftop level during the 5-minute time periods identified as combustion-related (3.2% of 5-minute periods), we observed a median slope of 0.011 $\frac{ppbv\ N_2O}{ppbv\ CO}$ (Inter-quartile range: 0.007, 0.024) (Figure 2C). These periods accounted for 5.0% of N_2O enhancements above background. We observed this relationship in all wind directions, confirming that this source was a distributed, non-point source and consistent with the presence of traffic in all directions. The similarity in N_2O/CO ratios between the street-level and tower-level combustion plumes were used to identify traffic-related signals at rooftop level.

The EDGARv2024 inventory indicates traffic-related emissions comprise 23% of N_2O emissions in the NYC region, with other combustion-related emissions comprise an additional 43% (e.g. residential combustion or energy production that may

https://doi.org/10.5194/egusphere-2026-3919
Preprint. Discussion started: 3 August 2026

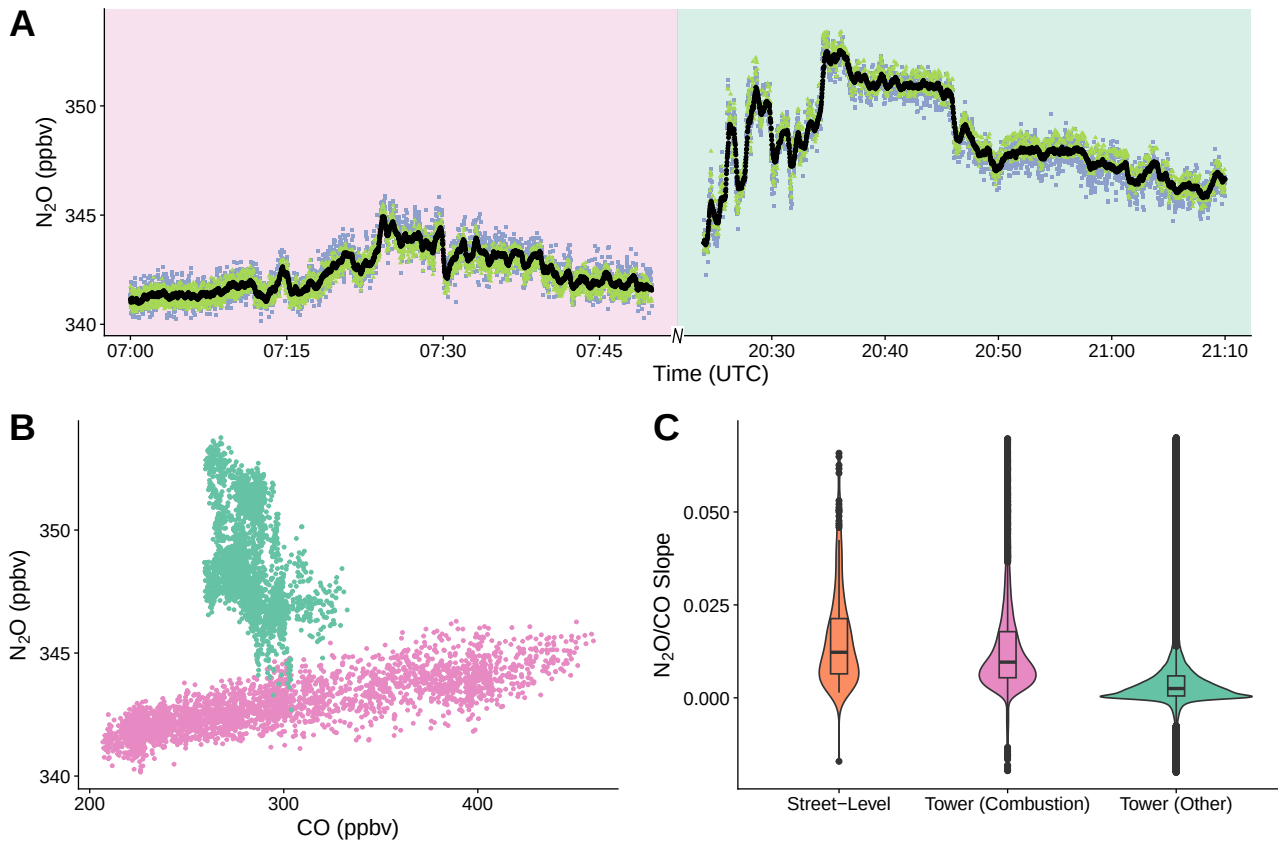

Figure 2. A) Tower-based time series showing two plumes as the appear on all three analyzers (Aerodyne SuperDUAL - Black; LI-7820 - Green; Aeris MIRA Ultra - Blue). We identify the first time series as combustion-related (pink in B and C) and the second as a non-combustion signal (green in B and C). B) Scatterplot of the N_2O and CO for the same two plumes as in A. C) Violin plot comparing the distribution of N_2O/CO ratios found in the times identified as combustion signal at rooftop level (pink, Aerodyne SuperDUAL) with the signal found from the mobile surveys (orange; Aeris MIRA Ultra). All non-combustion related tower times are shown in green.

https://doi.org/10.5194/egusphere-2026-3919
Preprint. Discussion started: 3 August 2026

also emit CO). We expect atmospheric mixing of both N_2O and CO from other sources at the tower level, meaning the observed fraction of enhancements associated with combustion was not indicative of the fraction of combustion-related emissions. However, the large discrepancy between the observations and EDGARv2024 combined with large observed enhancements associated with wastewater treatment (see below) indicate that combustion-related emissions likely account for a smaller fraction of N_2O emissions than the 66% in EDGARv2024. This is consistent with Forster et al. (2026), who found no significant rush hour peak of N_2O and a lower than expected correlation between N_2O and CO.

3.2.2 Wastewater Treatment Plants

Observations from tower level indicate that the largest N_2O enhancements come from the southeast of the CUNY site in the direction associated with Wards Island WWTP (see Supporting Information S6). The largest plumes were also typically associated with this wind direction, though others were observed in the direction of the Edgewater WWTP to the west of the site. As part of the 2022 campaign with the University of Albany, we drove loops around some of the largest WWTP in NYC and observed by far the largest enhancements (over 600 ppbv) around the Ward Island WWTP (Figure 3). These enhancements were far larger than any observed at other WWTP in the region or during the TEEMS campaign. The location of the Wards Island WWTP on an island meant our drives came too close to the plant for quantification of the emissions, but the large enhancements just outside of the plant were consistent with the observations at tower level. Wards Island WWTP serves over one million people and, unlike most other plants in NYC, uses biological nutrient removal technology, which is associated with N_2O emissions (Desloover et al., 2012; Law et al., 2012; Massara et al., 2017). Furthermore, Wards Island houses dewatering equipment for the sludge produced at several other NYC WWTP. Since sludge storage and dewatering produce N_2O emissions, we expect this site to emit more N_2O than other WWTPs in NYC. However, we did not observe significant N_2O enhancements around a second plant with dewatering equipment, Newtown Creek WWTP, which also serves over one million people. Newtown Creek WWTP was recently the site of a $5 billion upgrade that may have reduced emissions and does not use biological nutrient removal.

3.2.3 City-Scale Emissions

We consistently observed larger enhancements of N_2O than predicted from HRRR-STILT convolved with EDGARv2024. Hours with negative observed enhancements are expected given the purposefully conservative choice of background (see Supporting Information S2). The poor correlation between the observed and predicted enhancements for each hour reflects transport model error, the coarseness of the EDGARv2024 inventory, and emissions variability. A similar setup has shown better agreement in the past for CO (Schiferl et al., 2024) and methane (Schiferl et al., 2025) at the same site. Therefore, we average across hours to account for emissions variability and any unbiased transport errors. In only two months out of 32 was the mean observed enhancement lower than the mean predicted enhancement. Across all data, the mean observed enhancement was 3.3 times the predicted enhancement. Results from each sites differ (CUNY: 3.2, Rutgers: 2.2, FBF: 4.2) but all agree that the predicted enhancements were significantly lower than observed. The mean ratio of observed to predicted enhancements was slightly lower when using meteorology from NAM3 (see Supporting Information S3). We conclude that

https://doi.org/10.5194/egusphere-2026-3919
Preprint. Discussion started: 3 August 2026

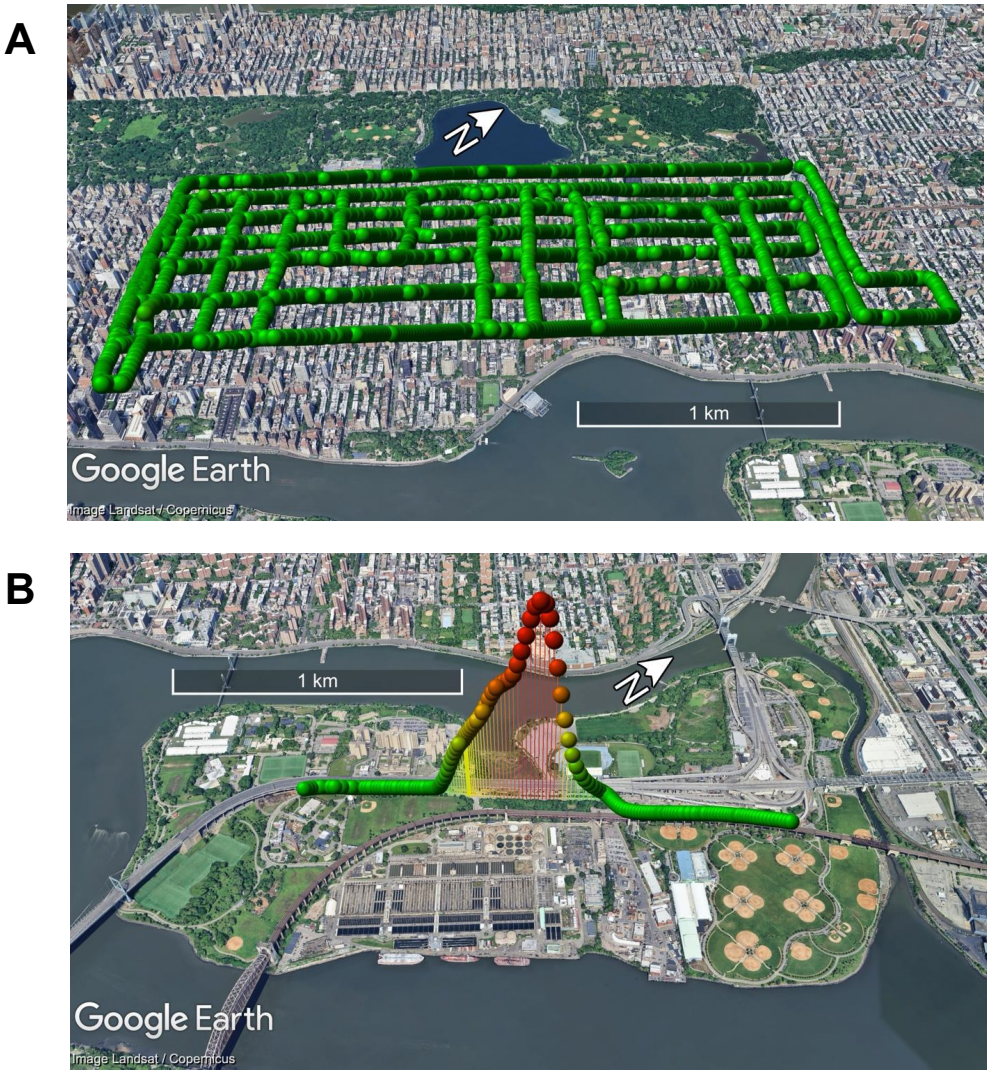

Figure 3. Maps of the mobile measurements targeting sources of N_2O using the Aeris MIRA Ultra analyzer. The height and color of points are determined by the N_2O mole fraction, with red representing mole fractions above 450 ppbv. A) The TEEMS campaign targeting the Upper East Side found much smaller enhancements that were typically related to combustion from traffic (2025-06-06). B) The mobile deployment around Wards Island found enhancements up to 900 ppbv around Wards Island WWTP on a day with wind from the East (2024-01-30). Since the image is 3-dimensional, scale bars are valid for their location on the map. © Google Earth. All rights reserved. Image taken from Google Earth Pro v7.3.7, 2026. 40°47'24.50"N, 73°55'27.23"W. Accessed 18 June 2026. Available at: earth.google.com. Landsat imagery courtesy of the U.S. Geological Survey.

https://doi.org/10.5194/egusphere-2026-3919
Preprint. Discussion started: 3 August 2026

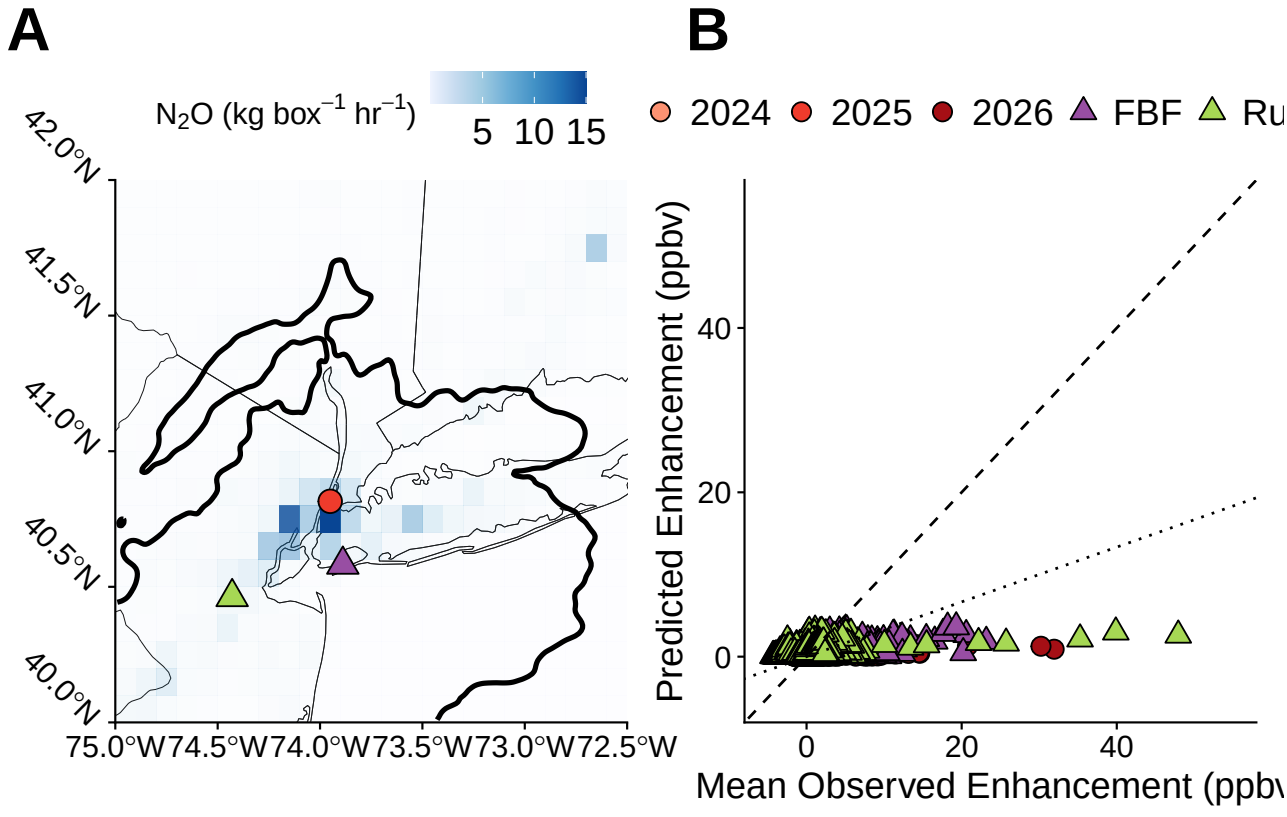

Figure 4. A) EDGARv2024 inventory for the NYC region plotted in blue. The 50th percentile of surface influence from the HRRR-STILT footprints (a measure of the region our sites are sensitive to emissions from) is shown with a black outline. Sites for our measurements are shown with the same symbols as in panel B). B) Hourly predicted and observed N_2O enhancements (in ppbv) between 11:00 and 16:00 local time. Predicted enhancements were calculated from HRRR-STILT convolved with the EDGARv2024 inventory. Hourly observations for 2024, 2025, and 2026 from the Aerodyne SuperDUAL at the CUNY site are shown in shades of red, while the FBF (July - December 2025; purple triangles) and Rutgers (June - September 2024; green triangles) deployments used the Aeris MIRA Ultra. The dashed line represents 1:1 while the dotted line represents 1:3. Due to the large number of points we have omitted error bars. The background-related uncertainty was around 8% of the total enhancement, while the standard deviation of N_2O mole fractions observed in each hour was typically around 40% of the enhancement.

https://doi.org/10.5194/egusphere-2026-3919
Preprint. Discussion started: 3 August 2026

the difference between the observed and N_2O emissions from the NYC region are most likely underestimated by a factor of 3, which is itself likely an underestimate due to the conservative choice of background percentile (see Supporting Information S2). We also note that this consistent underestimation likely indicates that N_2O is underestimated across the NYC region and that no one source is responsible for the underestimation. However, at all three sites the largest enhancements typically had no association with combustion tracer CO, again suggesting that wastewater treatment may be the main cause of the discrepancy. Another possible explanation are natural sources, such as soils, that do not appear in the anthropogenic-only EDGARv2024 inventory. Previous work has identified soils in NYC as a source of N_2O but did not quantify total emissions (Pierre et al., 2016). However, soils most likely had a more evenly distributed emission, which would be inconsistent with the significant dependence of enhancements on wind direction at the CUNY site.

4 Conclusions and Recommendations

We evaluated three commercially available laser-based spectrometers (Aerodyne SuperDUAL, Aeris MIRA Ultra, and LI-COR LI-7820) measuring N_2O for suitability in urban measurements. We assessed the analyzer precision, humidity sensitivity, and stability of all three analyzers. The Aerodyne SuperDUAL has the highest precision of the analyzers but requires consistent calibration, potentially even hourly, and expert maintenance for best results. This analyzer is also the largest of the three tested, requiring an external pump and chiller, and therefore is not suitable for smaller mobile vehicles. The Aeris MIRA Ultra has the least precision of the three analyzers and more frequent calibration does not improve uncertainty as much as for the other analyzers. The LI-7820 had the lowest calibration-related uncertainty when calibrating the analyzers daily, but the residual humidity dependence was difficult to correct. The LI-7820 has an internal battery that makes it ideal for portable applications or mobile sampling but it does not measure carbon monoxide (CO), which can distinguish between different sources of N_2O in urban environments. We recommend the Aerodyne SuperDUAL for the most precise applications and the LI-7820 for its flexibility, though the lack of a CO measurement is a significant drawback.

Using the data from the Aerodyne SuperDUAL and Aeris MIRA Ultra, we characterized N_2O emissions from the New York City region. Enhancements at three different sites were three times larger than predicted using the best available inventory, EDGARv2024, convolved with an atmospheric transport model (HRRR-STILT). Using the correlation with CO measurements from the same analyzers, we identified that traffic and other combustion-related emissions account for a lower fraction of emissions than indicated in the inventory. The largest enhancements were linked to specific wastewater treatment plants, especially the Wards Island Wastewater Treatment Plant. We confirmed our source identification with mobile measurements, finding much larger enhancements outside an older wastewater treatment plant than driving along city streets.

We found that the New York City region emits 3 times more N_2O than estimated in inventories, consistent with similar work in Los Angeles (Addington et al., 2021) and Rotterdam (Tong et al., 2023, 2025) but a larger underestimate than observations in Zurich (Harris et al., 2017) and Groningen (Tong et al., 2025). To understand whether other urban areas are similarly underestimated, we recommend tower and mobile measurements of N_2O using fast response laser-based spectrometers to capture the high variability of N_2O mole fractions observed here.

https://doi.org/10.5194/egusphere-2026-3919
Preprint. Discussion started: 3 August 2026

5 Supporting Information

Additional materials regarding methods, results, and discussion.

Data availability. Data used in this work are available at https://doi.org/10.5061/dryad.n5tb2rcbd

Author contributions. AHD, YZ, and RC designed the study. AHD performed the tests and tower deployments with help from all other authors. RD and RC performed the mobile deployment. AHD and RD analyzed the data. AHD prepared the manuscript with input from all other authors.

Competing interests. The authors declare that they have no competing or financial interests.

Acknowledgements. The authors would like to thank New York State Energy Research Development Agency for supporting this work (contract #183867). We thank LI-COR Environmental for loaning us the LI-7820 used in this paper and Ricardo Toledo-Crow and the Next Generation Environmental Sciences Observatory of the Advanced Sciences Research Center, City University of New York, for observatory space while conducting the instrument tests and tower deployment. We also thank Matt Drews from Rutgers University for hosting the site at Rutgers University and Elizabeth Stoehr from the Jamaica Bay-Rockaway Parks Conservancy for hosting the Floyd Bennett Field site. We also thank Mira Modi for help with the TEEMS mobile measurement campaign.

https://doi.org/10.5194/egusphere-2026-3919
Preprint. Discussion started: 3 August 2026

References

Addington, O., Zeng, Z.-C., Pongetti, T., Shia, R.-L., Gurney, K. R., Liang, J., Roest, G., He, L., Yung, Y. L., and Sander, S. P.: Estimating nitrous oxide (N2O) emissions for the Los Angeles Megacity using mountaintop remote sensing observations, Remote Sensing of Environment, 259, 112 351, https://doi.org/10.1016/j.rse.2021.112351, 2021.

Ammoura, L., Xueref-Remy, I., Vogel, F., Gros, V., Baudic, A., Bonsang, B., Delmotte, M., Té, Y., and Chevallier, F.: Exploiting stagnant conditions to derive robust emission ratio estimates for CO_2 , CO and volatile organic compounds in Paris, Atmospheric Chemistry and Physics, 16, 15 653–15 664, https://doi.org/10.5194/acp-16-15653-2016, 2016.

Aumer, W., Möller, M., Görres, C.-M., Eckhardt, C., Weber, T. K. D., Bilibio, C., Bruns, C., Gattinger, A., Finckh, M. R., and Kammann, C.: Technical note: Gas Chromatography vs. Mid-Infrared Laser Absorption Spectroscopy: A comparison of methods for measuring greenhouse gas fluxes from arable soils, https://doi.org/10.5194/egusphere-2025-2862, 2025.

Bai, X., Cripps, T., Serra, J., Butterbach-Bahl, K., and Yao, Z.: Spatial and temporal variability of CO_2 , N_2 O and CH_4 fluxes from an urban park in Denmark, https://doi.org/10.5194/egusphere-2025-5091, 2025.

Barker, P. A., Allen, G., Flynn, M., Riddick, S., and Pitt, J. R.: Measurement of recreational N2O emissions from an urban environment in Manchester, UK, Urban Climate, 46, 101 282, https://doi.org/10.1016/j.uclim.2022.101282, 2022.

Benjamin, S. G., Weygandt, S. S., Brown, J. M., Hu, M., Alexander, C. R., Smirnova, T. G., Olson, J. B., James, E. P., Dowell, D. C., Grell, G. A., Lin, H., Peckham, S. E., Smith, T. L., Moninger, W. R., Kenyon, J. S., and Manikin, G. S.: A North American Hourly Assimilation and Model Forecast Cycle: The Rapid Refresh, Monthly Weather Review, 144, 1669–1694, https://doi.org/10.1175/MWR-D-15-0242.1, 2016.

Bergamaschi, P., Corazza, M., Karstens, U., Athanassiadou, M., Thompson, R. L., Pison, I., Manning, A. J., Bousquet, P., Segers, A., Vermeulen, A. T., Janssens-Maenhout, G., Schmidt, M., Ramonet, M., Meinhardt, F., Aalto, T., Haszpra, L., Moncrieff, J., Popa, M. E., Lowry, D., Steinbacher, M., Jordan, A., O'Doherty, S., Piacentino, S., and Dlugokencky, E.: Top-down estimates of European CH_4 and N_2 O emissions based on four different inverse models, Atmospheric Chemistry and Physics, 15, 715–736, https://doi.org/10.5194/acp-15-715-2015, 2015.

Brannon, E. Q., Moseman-Valtierra, S. M., Rella, C. W., Martin, R. M., Chen, X., and Tang, J.: Evaluation of laser-based spectrometers for greenhouse gas flux measurements in coastal marshes, Limnology and Oceanography: Methods, 14, 466–476, https://doi.org/10.1002/lom3.10105, 2016.

Catena, A. M., Murray, L. T., Zhang, J., Leibensperger, E. M., Commane, R., Smith, M. L., Schwab, M. J., Hallward-Driemeier, A., Loman, M. L., and Schwab, J. J.: Intercomparison of Methane Emission Rate Methods Using Aerial and Ground-Level Mobile Monitoring at New York State Landfills, ACS ES&T Air, 3, 16–29, https://doi.org/10.1021/acsestair.5c00145, 2026.

Charoenpornpukdee, K., Stanley, K., Pitt, J., Wenger, A., Manning, A., Young, D., Say, D., and O'Doherty, S.: Recreational drug-use as an urban source of nitrous oxide, Environmental Science: Atmospheres, 3, 962–969, https://doi.org/10.1039/D3EA00025G, 2023.

Chu, M., Brimblecombe, P., Gali, N. K., Ghadikolaei, M. A., Wei, P., Li, X., Yang, S., Wei, Y., and Ning, Z.: Roadside measurement of N2O and CH4 emissions from vehicles in Hong Kong, Science of The Total Environment, 956, 177 241, https://doi.org/10.1016/j.scitotenv.2024.177241, 2024.

Commane, R., Hallward-Driemeier, A., and Murray, L. T.: Intercomparison of commercial analyzers for atmospheric ethane and methane observations, Atmospheric Measurement Techniques, 16, 1431–1441, https://doi.org/10.5194/amt-16-1431-2023, 2023.

https://doi.org/10.5194/egusphere-2026-3919
Preprint. Discussion started: 3 August 2026

Crippa, M., Guizzardi, D., Pagani, F., Banja, M., Muntean, M., Schaaf, E., Monforti-Ferrario, F., Becker, W., Quadrelli, R., Risquez Martin, A., Taghavi-Moharamli, P., Koykka, J., Grassi, G., Rossi, S., Melo, J., Oom, D., Branco, A., San-Miguel, J., Manca, G., Pisoni, E., Vignati, E., and Pekar, F.: GHG emissions of all world countries., Publications Office, LU, https://doi.org/10.2760/4002897, 2024.

Crutzen, P. J.: The influence of nitrogen oxides on the atmospheric ozone content, Quarterly Journal of the Royal Meteorological Society, 96, 320–325, https://doi.org/10.1002/qj.49709640815, 1970.

Defratyka, S. M., Paris, J.-D., Yver-Kwok, C., Loeb, D., France, J., Helmore, J., Yarrow, N., Gros, V., and Bousquet, P.: Ethane measurement by Picarro CRDS G2201-i in laboratory and field conditions: potential and limitations, Atmospheric Measurement Techniques, 14, 5049–5069, https://doi.org/10.5194/amt-14-5049-2021, 2021.

Desloover, J., Vlaeminck, S. E., Clauwaert, P., Verstraete, W., and Boon, N.: Strategies to mitigate N2O emissions from biological nitrogen removal systems, Current Opinion in Biotechnology, 23, 474–482, https://doi.org/10.1016/j.copbio.2011.12.030, 2012.

Fasoli, B., Lin, J. C., Bowling, D. R., Mitchell, L., and Mendoza, D.: Simulating atmospheric tracer concentrations for spatially distributed receptors: updates to the Stochastic Time-Inverted Lagrangian Transport model's R interface (STILT-R version 2), https://doi.org/10.5194/gmd-2018-20, 2018.

Floerchinger, C., Shepson, P. B., Hajny, K., Daube, B. C., Stirm, B. H., Sweeney, C., and Wofsy, S. C.: Relative flux measurements of biogenic and natural gas-derived methane for seven U.S. cities, Elementa: Science of the Anthropocene, 9, 000 119, https://doi.org/10.1525/elementa.2021.000119, 2021.

Forster, G., Biggart, M., Doherty, R. M., Baker, A. R., Etchells, A., Mills, G., Thi Hien, T., Chi, N. D. T., Huy, D. H., and Oram, D.: A significant source of nitrous oxide from recreational use in Ho Chi Minh City, a future Southeast Asian megacity in Vietnam, Environmental Science: Atmospheres, 6, 390–404, https://doi.org/10.1039/D5EA00083A, 2026.

Forster, P., Storelvmo, T., Armour, K., Collins, W., Dufresne, J.-L., Frame, D., Lunt, D., Mauritsen, T., Palmer, M., Watanabe, M., Wild, M., and Zhang, H.: The Earth's Energy Budget, Climate Feedbacks, and Climate Sensitivity, in: Climate Change 2021 – The Physical Science Basis: Working Group I Contribution to the Sixth Assessment Report of the Intergovernmental Panel on Climate Change, pp. 923–1054, Cambridge University Press, 1 edn., ISBN 978-1-009-15789-6, https://doi.org/10.1017/9781009157896, 2023.

Fries, A. E., Schifman, L. A., Shuster, W. D., and Townsend-Small, A.: Street-level emissions of methane and nitrous oxide from the wastewater collection system in Cincinnati, Ohio, Environmental Pollution, 236, 247–256, https://doi.org/10.1016/j.envpol.2018.01.076, 2018.

Ganesan, A. L., Manning, A. J., Grant, A., Young, D., Oram, D. E., Sturges, W. T., Moncrieff, J. B., and O'Doherty, S.: Quantifying methane and nitrous oxide emissions from the UK and Ireland using a national-scale monitoring network, Atmospheric Chemistry and Physics, 15, 6393–6406, https://doi.org/10.5194/acp-15-6393-2015, 2015.

Gonzalez, Y., Commane, R., Manninen, E., Daube, B. C., Schiferl, L. D., McManus, J. B., McKain, K., Hintsa, E. J., Elkins, J. W., Montzka, S. A., Sweeney, C., Moore, F., Jimenez, J. L., Campuzano Jost, P., Ryerson, T. B., Bourgeois, I., Peischl, J., Thompson, C. R., Ray, E., Wennberg, P. O., Crounse, J., Kim, M., Allen, H. M., Newman, P. A., Stephens, B. B., Apel, E. C., Hornbrook, R. S., Nault, B. A., Morgan, E., and Wofsy, S. C.: Impact of stratospheric air and surface emissions on tropospheric nitrous oxide during ATom, Atmospheric Chemistry and Physics, 21, 11 113–11 132, https://doi.org/10.5194/acp-21-11113-2021, 2021.

Gålfalk, M. and Bastviken, D.: In Situ Observations Reveal Underestimated Greenhouse Gas Emissions from Wastewater Treatment with Anaerobic Digestion – Sludge Was a Major Source for Both CH_4 and N_2 O, Environmental Science & Technology, 59, 18 146–18 155, https://doi.org/10.1021/acs.est.5c04780, 2025.

https://doi.org/10.5194/egusphere-2026-3919
Preprint. Discussion started: 3 August 2026

Gålfalk, M., Påledal, S. N., Sehlén, R., and Bastviken, D.: Ground-based remote sensing of CH4 and N2O fluxes from a wastewater treatment plant and nearby biogas production with discoveries of unexpected sources, Environmental Research, 204, 111 978, https://doi.org/10.1016/j.envres.2021.111978, 2022.

Harris, E., Henne, S., Hüglin, C., Zellweger, C., Tuzson, B., Ibraim, E., Emmenegger, L., and Mohn, J.: Tracking nitrous oxide emission processes at a suburban site with semicontinuous, in situ measurements of isotopic composition, Journal of Geophysical Research: Atmospheres, 122, 1850–1870, https://doi.org/10.1002/2016JD025906, 2017.

Haszpra, L., Hidy, D., Taligás, T., and Barcza, Z.: First results of tall tower based nitrous oxide flux monitoring over an agricultural region in Central Europe, Atmospheric Environment, 176, 240–251, https://doi.org/10.1016/j.atmosenv.2017.12.035, 2018.

Herrera, S. A., Diskin, G. S., Harward, C., Sachse, G., De Wekker, S. F. J., Yang, M., Choi, Y., Wisthaler, A., Mallia, D. V., and Pusede, S. E.: Wintertime Nitrous Oxide Emissions in the San Joaquin Valley of California Estimated from Aircraft Observations, Environmental Science & Technology, 55, 4462–4473, https://doi.org/10.1021/acs.est.0c08418, 2021.

Hoekman, S. K.: Review of Nitrous Oxide (N_2O) Emissions from Motor Vehicles, SAE International Journal of Fuels and Lubricants, 13, 79–98, https://doi.org/10.4271/04-13-01-0005, 2020.

Jimenez, J., McManus, J., Shorter, J., Nelson, D., Zahniser, M., Koplow, M., McRae, G., and Kolb, C.: Cross road and mobile tunable infrared laser measurements of nitrous oxide emissions from motor vehicles, Chemosphere - Global Change Science, 2, 397–412, https://doi.org/10.1016/S1465-9972(00)00019-2, 2000.

Järvi, L., Nordbo, A., Rannik, U., Haapanala, S., Riikonen, A., Mammarella, I., Pihlatie, M., and Vesala, T.: Urban nitrous-oxide fluxes measured using the eddy-covariance technique in Helsinki, Finland, Boreal Environment Research, 19, 14, 2014.

Kashtan, Y., Nicholson, M., Finnegan, C. J., Ouyang, Z., Garg, A., Lebel, E. D., Rowland, S. T., Michanowicz, D. R., Herrera, J., Nadeau, K. C., and Jackson, R. B.: Nitrogen dioxide exposure, health outcomes, and associated demographic disparities due to gas and propane combustion by U.S. stoves, Science Advances, 10, eadm8680, https://doi.org/10.1126/sciadv.adm8680, 2024.

Kashtan, Y. S., Nicholson, M., Finnegan, C., Ouyang, Z., Lebel, E. D., Michanowicz, D. R., Shonkoff, S. B., and Jackson, R. B.: Gas and Propane Combustion from Stoves Emits Benzene and Increases Indoor Air Pollution, Environmental Science & Technology, 57, 9653–9663, https://doi.org/10.1021/acs.est.2c09289, 2023.

Knez, L., Eckl, M., Waldmann, P., Fiehn, A., Pühl, M., Aseev, O., Diskin, G. S., DiGangi, J. P., Choi, Y., Miech, J. A., Bennett, R., Gatebe, C. K., Dean-Day, J. M., Poudyal, R., Lee, G., Kim, J., and Roiger, A.: Airborne performance assessment of the DLR MIRO MGA^3 quantum cascade laser spectrometer for fast N_2 O measurements, https://doi.org/10.5194/egusphere-2026-1686, 2026.

Kong, M., Mitu, F. F., Petersen, S. O., Lærke, P. E., Abalos, D., Sørensen, P., Brændholt, A., Bruun, S., Eriksen, J., and Dold, C.: A comparison of chamber-based methods for measuring N2O emissions from arable soils, Agricultural and Forest Meteorology, 370, 110 591, https://doi.org/10.1016/j.agrformet.2025.110591, 2025.

Kostinek, J., Roiger, A., Davis, K. J., Sweeney, C., DiGangi, J. P., Choi, Y., Baier, B., Hase, F., Groß, J., Eckl, M., Klausner, T., and Butz, A.: Adaptation and performance assessment of a quantum and interband cascade laser spectrometer for simultaneous airborne in situ observation of CH4, C2H6, CO2, CO and N2O, Atmospheric Measurement Techniques, 12, 1767–1783, https://doi.org/10.5194/amt-12-1767-2019, 2019.

Krebbers, R., Van Kempen, K., Lin, Y., Meurs, J., Hendriks, L., Aben, R., Paranaiba, J. R., Fritz, C., Veraart, A. J., Khodabakhsh, A., and Cristescu, S. M.: Ultra-broadband coherent open-path spectroscopy for multi-gas monitoring in wastewater treatment, Environmental Science and Ecotechnology, 25, 100 554, https://doi.org/10.1016/j.ese.2025.100554, 2025.

https://doi.org/10.5194/egusphere-2026-3919
Preprint. Discussion started: 3 August 2026

Law, Y., Ye, L., Pan, Y., and Yuan, Z.: Nitrous oxide emissions from wastewater treatment processes, Philosophical Transactions of the Royal Society B: Biological Sciences, 367, 1265–1277, https://doi.org/10.1098/rstb.2011.0317, 2012.

Lin, J. C., Gerbig, C., Wofsy, S. C., Andrews, A. E., Daube, B. C., Davis, K. J., and Grainger, C. A.: A near-field tool for simulating the upstream influence of atmospheric observations: The Stochastic Time-Inverted Lagrangian Transport (STILT) model, Journal of Geophysical Research: Atmospheres, 108, 2002JD003 161, https://doi.org/10.1029/2002JD003161, 2003.

Lopez-Coto, I., Ren, X., Karion, A., McKain, K., Sweeney, C., Dickerson, R. R., McDonald, B. C., Ahn, D. Y., Salawitch, R. J., He, H., Shepson, P. B., and Whetstone, J. R.: Carbon Monoxide Emissions from the Washington, DC, and Baltimore Metropolitan Area: Recent Trend and COVID-19 Anomaly, Environmental Science & Technology, 56, 2172–2180, https://doi.org/10.1021/acs.est.1c06288, 2022.

Massara, T. M., Malamis, S., Guisasola, A., Baeza, J. A., Noutsopoulos, C., and Katsou, E.: A review on nitrous oxide (N 2 O) emissions during biological nutrient removal from municipal wastewater and sludge reject water, Science of The Total Environment, 596-597, 106–123, https://doi.org/10.1016/j.scitotenv.2017.03.191, 2017.

McKain, K., Down, A., Raciti, S. M., Budney, J., Hutyra, L. R., Floerchinger, C., Herndon, S. C., Nehrkorn, T., Zahniser, M. S., Jackson, R. B., Phillips, N., and Wofsy, S. C.: Methane emissions from natural gas infrastructure and use in the urban region of Boston, Massachusetts, Proceedings of the National Academy of Sciences, 112, 1941–1946, https://doi.org/10.1073/pnas.1416261112, 2015.

Miller, S. M., Kort, E. A., Hirsch, A. I., Dlugokencky, E. J., Andrews, A. E., Xu, X., Tian, H., Nehrkorn, T., Eluszkiewicz, J., Michalak, A. M., and Wofsy, S. C.: Regional sources of nitrous oxide over the United States: Seasonal variation and spatial distribution, Journal of Geophysical Research: Atmospheres, 117, n/a–n/a, https://doi.org/10.1029/2011JD016951, 2012.

Moore, D. P., Li, N. P., Song, C., Zhu, J.-J., Yi, H., Tao, L., McSpiritt, J., Sevostianov, V. I., Wendt, L. P., Rojas-Robles, N. E., Hopkins, F. M., Ren, Z. J., and Zondlo, M. A.: Comprehensive assessment of the contribution of wastewater treatment to urban greenhouse gas and ammonia emissions, Nature Water, 3, 1114–1124, https://doi.org/10.1038/s44221-025-00490-z, 2025.

Oshita, K., Okumura, T., Takaoka, M., Fujimori, T., Appels, L., and Dewil, R.: Methane and nitrous oxide emissions following anaerobic digestion of sludge in Japanese sewage treatment facilities, Bioresource Technology, 171, 175–181, https://doi.org/10.1016/j.biortech.2014.08.081, 2014.

Peterse, I. F., Hendriks, L., Weideveld, S. T., Smolders, A. J., Lamers, L. P., Lücker, S., and Veraart, A. J.: Wastewater-effluent discharge and incomplete denitrification drive riverine CO2, CH4 and N2O emissions, Science of The Total Environment, 951, 175 797, https://doi.org/10.1016/j.scitotenv.2024.175797, 2024.

Pierre, S., Groffman, P. M., Killilea, M. E., and Oldfield, E. E.: Soil microbial nitrogen cycling and nitrous oxide emissions from urban afforestation in the New York City Afforestation Project, Urban Forestry & Urban Greening, 15, 149–154, https://doi.org/10.1016/j.ufug.2015.11.006, 2016.

Plant, G., Kort, E. A., Floerchinger, C., Gvakharia, A., Vimont, I., and Sweeney, C.: Large Fugitive Methane Emissions From Urban Centers Along the U.S. East Coast, Geophysical Research Letters, 46, 8500–8507, https://doi.org/10.1029/2019GL082635, 2019.

Prather, M. J., Hsu, J., DeLuca, N. M., Jackman, C. H., Oman, L. D., Douglass, A. R., Fleming, E. L., Strahan, S. E., Steenrod, S. D., Søvde, O. A., Isaksen, I. S. A., Froidevaux, L., and Funke, B.: Measuring and modeling the lifetime of nitrous oxide including its variability, Journal of Geophysical Research: Atmospheres, 120, 5693–5705, https://doi.org/10.1002/2015JD023267, 2015.

Ravishankara, A. R., Daniel, J. S., and Portmann, R. W.: Nitrous Oxide (N_2O): The Dominant Ozone-Depleting Substance Emitted in the 21st Century, Science, 326, 123–125, https://doi.org/10.1126/science.1176985, 2009.

Richardson, A. D., Kong, G. V., Taylor, K. M., Le Moine, J. M., Bowker, M. A., Barber, J. J., Basler, D., Carbone, M. S., Hayer, M., Koch, G. W., Salvatore, M. R., Sonnemaker, A. W., and Trilling, D. E.: Soil-atmosphere fluxes of CO2, CH4, and

https://doi.org/10.5194/egusphere-2026-3919
Preprint. Discussion started: 3 August 2026

N2O across an experimentally-grown, successional gradient of biocrust community types, Frontiers in Microbiology, 13, 979 825, https://doi.org/10.3389/fmicb.2022.979825, 2022.

Sargent, M., Barrera, Y., Nehrkorn, T., Hutyra, L. R., Gately, C. K., Jones, T., McKain, K., Sweeney, C., Hegarty, J., Hardiman, B., Wang, J. A., and Wofsy, S. C.: Anthropogenic and biogenic CO_2 fluxes in the Boston urban region, Proceedings of the National Academy of Sciences, 115, 7491–7496, https://doi.org/10.1073/pnas.1803715115, 2018.

Sargent, M. R., Floerchinger, C., McKain, K., Budney, J., Gottlieb, E. W., Hutyra, L. R., Rudek, J., and Wofsy, S. C.: Majority of US urban natural gas emissions unaccounted for in inventories, Proceedings of the National Academy of Sciences, 118, e2105804 118, https://doi.org/10.1073/pnas.2105804118, 2021.

Schiavina, M., Melchiorri, M., and Pesaresi, M.: GHS-SMOD R2023A - GHS settlement layers, application of the Degree of Urbanisation methodology (stage I) to GHS-POP R2023A and GHS-BUILT-S R2023A, multitemporal (1975-2030), https://doi.org/10.2905/A0DF7A6F-49DE-46EA-9BDE-563437A6E2BA, 2023.

Schiferl, L. D., Cao, C., Dalton, B., Hallward-Driemeier, A., Toledo-Crow, R., and Commane, R.: Multi-year observations of variable incomplete combustion in the New York megacity, Atmospheric Chemistry and Physics, 24, 10 129–10 142, https://doi.org/10.5194/acp-24-10129-2024, 2024.

Schiferl, L. D., Hallward-Driemeier, A., Zhao, Y., Toledo-Crow, R., and Commane, R.: Missing wintertime methane emissions from New York City related to combustion, Atmospheric Chemistry and Physics, 25, 15 683–15 700, https://doi.org/10.5194/acp-25-15683-2025, 2025.

Seuferling, C., Brye, K., Della Lunga, D., Brye, J., Daniels, M., Wood, L., and Greub, K.: Evaluation of Greenhouse Gas-Flux-Determination Models and Calculation in Southeast Arkansas Cotton Production, AgriEngineering, 7, 213, https://doi.org/10.3390/agriengineering7070213, 2025.

Song, C., Zhu, J.-J., Willis, J. L., Moore, D. P., Zondlo, M. A., and Ren, Z. J.: Oversimplification and misestimation of nitrous oxide emissions from wastewater treatment plants, Nature Sustainability, https://doi.org/10.1038/s41893-024-01420-9, 2024.

Szopa, S., Naik, V., Adhikary, B., Artaxo, P., Berntsen, T., Collins, W. D., Fuzzi, S., Gallardo, L., Kiendler-Scharr, A., Klimont, Z., Liao, H., Unger, N., and Zanis, P.: Short-lived Climate Forcers, in: Climate Change 2021: The Physical Science Basis. Contribution of Working Group I to the Sixth Assessment Report of the Intergovernmental Panel on Climate Change, pp. 817–922, Cambridge University Press, Cambridge, United Kingdom and New York, NY, USA, https://doi.org/10.1017/9781009157896.008, 2023.

Tian, H., Pan, N., Thompson, R. L., Canadell, J. G., Suntharalingam, P., Regnier, P., Davidson, E. A., Prather, M., Ciais, P., Muntean, M., Pan, S., Winiwarter, W., Zaehle, S., Zhou, F., Jackson, R. B., Bange, H. W., Berthet, S., Bian, Z., Bianchi, D., Bouwman, A. F., Buitenhuis, E. T., Dutton, G., Hu, M., Ito, A., Jain, A. K., Jeltsch-Thömmes, A., Joos, F., Kou-Giesbrecht, S., Krummel, P. B., Lan, X., Landolfi, A., Lauerwald, R., Li, Y., Lu, C., Maavara, T., Manizza, M., Millet, D. B., Mühle, J., Patra, P. K., Peters, G. P., Qin, X., Raymond, P., Resplandy, L., Rosentreter, J. A., Shi, H., Sun, Q., Tonina, D., Tubiello, F. N., Van Der Werf, G. R., Vuichard, N., Wang, J., Wells, K. C., Western, L. M., Wilson, C., Yang, J., Yao, Y., You, Y., and Zhu, Q.: Global nitrous oxide budget (1980–2020), Earth System Science Data, 16, 2543–2604, https://doi.org/10.5194/essd-16-2543-2024, 2024.

Tong, X., Van Heuven, S., Scheeren, B., Kers, B., Hutjes, R., and Chen, H.: Aircraft-Based AirCore Sampling for Estimates of N_2 O and CH_4 Emissions, Environmental Science & Technology, 57, 15 571–15 579, https://doi.org/10.1021/acs.est.3c04932, 2023.

Tong, X., Zhao, Z., Hensen, A., Bruin, G. J., Van Heuven, S., Scheeren, B., Hutjes, R., and Chen, H.: Toward Reconciling Bottom-Up and Top-Down Estimates of N_2 O and CH_4 Emissions in Rotterdam, Journal of Geophysical Research: Atmospheres, 130, e2025JD044 365, https://doi.org/10.1029/2025JD044365, 2025.

https://doi.org/10.5194/egusphere-2026-3919
Preprint. Discussion started: 3 August 2026

Townsend-Small, A., Pataki, D. E., Tseng, L. Y., Tsai, C.-Y., and Rosso, D.: Nitrous Oxide Emissions from Wastewater Treatment and Water Reclamation Plants in Southern California, Journal of Environmental Quality, 40, 1542–1550, https://doi.org/10.2134/jeq2011.0059, 2011.

Triches, N. Y., Engel, J., Bolek, A., Vesala, T., Marushchak, M. E., Virkkala, A.-M., Heimann, M., and Göckede, M.: Practical guidelines for reproducible N_2 O flux chamber measurements in nutrient-poor ecosystems, Atmospheric Measurement Techniques, 18, 3407–3424, https://doi.org/10.5194/amt-18-3407-2025, 2025.

Vasilaki, V., Massara, T., Stanchev, P., Fatone, F., and Katsou, E.: A decade of nitrous oxide (N2O) monitoring in full-scale wastewater treatment processes: A critical review, Water Research, 161, 392–412, https://doi.org/10.1016/j.watres.2019.04.022, 2019.

Wei, D., Reinmann, A., Schiferl, L. D., and Commane, R.: High resolution modeling of vegetation reveals large summertime biogenic CO_2 fluxes in New York City, Environmental Research Letters, 17, 124 031, https://doi.org/10.1088/1748-9326/aca68f, 2022.

Willén, A., Rodhe, L., Pell, M., and Jönsson, H.: Nitrous oxide and methane emissions during storage of dewatered digested sewage sludge, Journal of Environmental Management, 184, 560–568, https://doi.org/10.1016/j.jenvman.2016.10.025, 2016.

Wunch, D., Wennberg, P. O., Toon, G. C., Keppel-Aleks, G., and Yavin, Y. G.: Emissions of greenhouse gases from a North American megacity, Geophysical Research Letters, 36, 2009GL039 825, https://doi.org/10.1029/2009GL039825, 2009.

Xiang, B., Miller, S. M., Kort, E. A., Santoni, G. W., Daube, B. C., Commane, R., Angevine, W. M., Ryerson, T. B., Trainer, M. K., Andrews, A. E., Nehrkorn, T., Tian, H., and Wofsy, S. C.: Nitrous oxide (N_2 O) emissions from California based on 2010 CalNex airborne measurements, Journal of Geophysical Research: Atmospheres, 118, 2809–2820, https://doi.org/10.1002/jgrd.50189, 2013.

Yacovitch, T. I., Herndon, S. C., Roscioli, J. R., Floerchinger, C., McGovern, R. M., Agnese, M., Pétron, G., Kofler, J., Sweeney, C., Karion, A., Conley, S. A., Kort, E. A., Nähle, L., Fischer, M., Hildebrandt, L., Koeth, J., McManus, J. B., Nelson, D. D., Zahniser, M. S., and Kolb, C. E.: Demonstration of an Ethane Spectrometer for Methane Source Identification, Environmental Science & Technology, 48, 8028–8034, https://doi.org/10.1021/es501475q, 2014.

Yang, Y., Yuan, X., Yu, L., Jong, M.-C., Pius, O., Zou, N., Zuo, Z., Yang, J., and Zuo, J.: Assessment of methane and nitrous oxide emissions from urban community sewer networks: Field quantification and insights into environmental factors, Water Research X, 28, 100 307, https://doi.org/10.1016/j.wroa.2025.100307, 2025.

Yver Kwok, C., Laurent, O., Guemri, A., Philippon, C., Wastine, B., Rella, C. W., Vuillemin, C., Truong, F., Delmotte, M., Kazan, V., Darding, M., Lebègue, B., Kaiser, C., Xueref-Rémy, I., and Ramonet, M.: Comprehensive laboratory and field testing of cavity ring-down spectroscopy analyzers measuring H_2 O, CO_2 , CH_4 and CO, Atmospheric Measurement Techniques, 8, 3867–3892, https://doi.org/10.5194/amt-8-3867-2015, 2015.

Zhan, Y., Yao, Z., Groffman, P. M., Xie, J., Wang, Y., Li, G., Zheng, X., and Butterbach-Bahl, K.: Urbanization can accelerate climate change by increasing soil N2O emission while reducing CH4 uptake, Global Change Biology, 29, 3489–3502, https://doi.org/10.1111/gcb.16652, 2023.